



5th International Conference on Energy and Environment Research, ICEER 2018

## Simulation of explosion characteristics of syngas/air mixtures

Manh-Vu Tran<sup>a,\*</sup>, Gianfranco Scribano<sup>b</sup>, Cheng Tung Chong<sup>c</sup>, Think X. Ho<sup>d</sup>

<sup>a</sup>*School of Engineering, Monash University Malaysia, Jalan Lagoon Selatan, 47500 Bandar Sunway, Selangor, Malaysia*

<sup>b</sup>*Department of Mechanical, Materials and Manufacturing Engineering, The University of Nottingham Malaysia Campus, Jalan Broga, 43500 Semenyih, Selangor, Malaysia*

<sup>c</sup>*UTM Centre for Low Carbon Transport in cooperation with Imperial College London, Universiti Teknologi Malaysia, 81310 Skudai, Johor, Malaysia*

<sup>d</sup>*Faculty of Engineering, Vietnamese - German University, Le Lai Street, Hoa Phu, Thu Dau Mot, Binh Duong, Vietnam*

---

### Abstract

Explosion characteristics of syngas/air mixtures was investigated numerically in a 3-D cylindrical geometric model, using ANSYS Fluent. The results showed that the maximum explosion pressure increased from lean to an equivalence ratio of 1.2, then decreased significantly with richer mixtures, indicating that maximum explosion pressure occurred at the equivalence ratio of 1.2, while explosion time was shortest at an equivalence ratio of 1.6. Increasing H<sub>2</sub> content in the fuel blends raised maximum explosion pressure and significantly shortened the explosion time. Normalized peak pressure was sensitive to the initial pressure of the mixture, showing that they significantly changed with increased initial pressure.

© 2018 The Authors. Published by Elsevier Ltd.

This is an open access article under the CC BY-NC-ND license (<https://creativecommons.org/licenses/by-nc-nd/4.0/>)

Selection and peer-review under responsibility of the scientific committee of the 5th International Conference on Energy and Environment Research, ICEER 2018.

*Keywords:* Explosion time; maximum explosion pressure; numerical simulation; syngas.

---

### 1. Introduction

Recently, syngas has emerged as the likely candidate for greener energy conversion since it possesses numerous advantages in stationary power generation [1]. In transportation, storage and fuel usage, explosion is a serious hazard

---

\* Corresponding author. Tel.: +60-355144420.

E-mail address: [manhvu.tran@monash.edu](mailto:manhvu.tran@monash.edu)

that causes injury and damage to its surroundings. When such an explosion takes place in a closed chamber, without proper venting or suppressing devices, it can damage the combustion chamber. To prevent such incidents, it is necessary to understand fuel explosion behavior and its proper use.

Computational fluid dynamics (CFD) coupled to chemical mechanism has been revealed as a numerical simulation technique to predict combustion performance resulting from physical and chemical processes of a flame. Among commercial softwares, ANSYS Fluent has been widely used to solve complex compressible and non-compressible fluid flows, including simulation of the combustion process in a closed chamber [2].

In this study, the explosion behaviors of syngas/air mixtures were numerically investigated at various equivalence ratios, H<sub>2</sub>:CO ratios, and initial pressures, using ANSYS Fluent software, subsequently a simulation method to estimate the explosion hazard of a syngas/air mixture in a confined space is proposed.

## 2. Numerical simulation

The analysis of a gaseous explosion process in a cylindrical chamber was conducted by means of a finite-volume CFD three dimensional model, based on the unsteady Reynolds Averaged Navier Stokes approach. A 3-D cylindrical geometry model, with a diameter of 20 cm and a length of 22 cm, was generated. The gaseous explosion process followed conservations of mass, momentum, energy and chemical components.

The conservation of mass is

$$\frac{\partial \rho}{\partial t} + \frac{\partial}{\partial x_j}(\rho u_j) = 0 \quad (1)$$

where  $x_j$  is the space coordinate in the direction  $j$ ,  $t$  is the time,  $\rho$  is the density, and  $u_j$  is the velocity component along the direction  $j$ .

The conservation of momentum is

$$\frac{\partial}{\partial t}(\rho u_i) + \frac{\partial}{\partial x_j}(\rho u_j u_i) = -\frac{\partial p}{\partial x_i} + \frac{\partial \tau_{ij}}{\partial x_j} \quad (2)$$

where  $p$  is the fluid pressure and  $\tau_{ij}$  is the stress tensor.

The conservation of energy is

$$\frac{\partial}{\partial t}(\rho E) + \frac{\partial}{\partial x_j}(\rho u_j E) = -\frac{\partial}{\partial x_j}(p u_j) + \frac{\partial}{\partial x_j}(\tau_{ij} u_j) - \frac{\partial q_j}{\partial x_j} + S_E \quad (3)$$

where  $S_E$  is a source of energy,  $q_j$  is heat flux,  $E$  is expressed as  $E = e + \frac{1}{2} u_i u_i$ , with  $e$  the internal energy per unit mass.

The conservation of chemical species is

$$\frac{\partial}{\partial t}(\rho Y_i) + \frac{\partial}{\partial x_j}(\rho u_j Y_i) = -\frac{\partial J_i}{\partial x_j} + R_i \quad (4)$$

where  $Y_i$  is the mass fraction,  $J_i$  is the diffusion flux, and  $R_i$  is the rate of generation of chemical species  $i$ .

For the turbulence closure model, the realizable  $k-\varepsilon$  model, incorporating the solution of transport equations for the turbulent kinetic energy and its dissipation rate, was chosen. The laminar finite-rate model was used to compute chemical source terms. The optimized H<sub>2</sub>/CO mechanism of Davis et al. [3], with 14 species and 30 reactions, was used. For density, the ideal gas law was selected. The transport property of pure species was determined based on the molecular kinetic theory; and the specific heat capacity of pure species was evaluated with piecewise temperature

polynomials. The momentum term was treated with a second-order upwind scheme, and the pressure and velocity were solved with a SIMPLEC algorithm [2]. All of the governing equations were solved with the unsteady solver available in ANSYS Fluent 16.2.

A structured mesh, with hexahedral elements for the internal fluid field, was generated using ICEM CFD. Figure 1a shows the computational domain with 255,000 total cells and grid spacing of 4 mm. The only boundary condition was the temperature on the wall, which was set to 298 K; during the short sequence of the explosion, the wall temperature could not rise substantially. The wall thickness was set at 0.01 m and the material used was stainless steel.

The initial conditions were the mass fraction of the mixture,  $H_2$ , CO,  $O_2$ , and  $N_2$ , which were changed to correspond with the equivalence ratio. The initial temperature of the mixture was 298 K and the pressure in the chamber was varied to match the experimental conditions.

A sphere patching region of 3 mm radius, with a temperature of 1500 K, was located at the center of the geometry to ignite the combustible mixture. The pressure value was monitored at a point on the wall (Fig. 1b), to match with the pressure transducer location in the experiment. Data were collected every ten time steps with  $2e^{-5}$  sec for each time step. Figure 1c shows an initial temperature field, which is a small high-temperature-regime, located at the center of the 3-D cylindrical geometry.

### 3. Results and discussion

#### 3.1. Temperature and velocity distributions in propagating flame

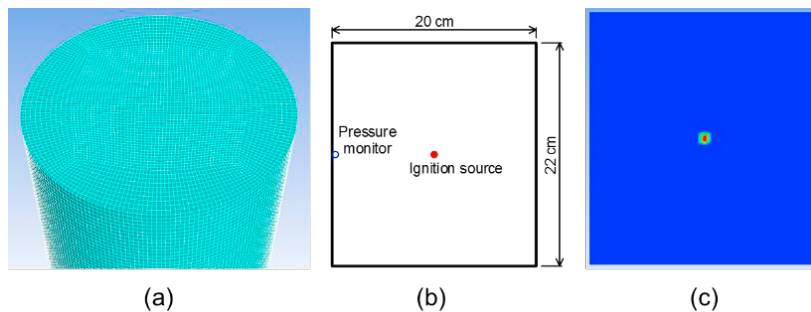


Fig. 1. CFD model for simulating the explosion, (a) Mesh of internal fluid, (b) Schematic diagram of chamber, (c) Initial temperature field.

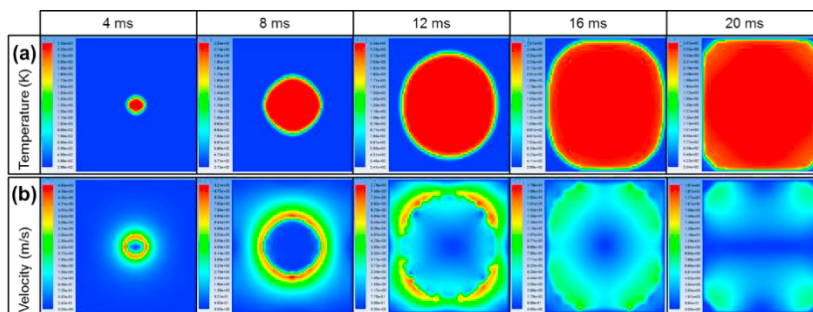


Fig. 2. Simulated (a) temperature and (b) velocity contours of  $50H_2:50CO/air$  propagating flame at  $P_u = 0.1$  MPa and  $\phi = 0.8$ .

Figure 2 shows variations of the simulated temperature and velocity fields of  $50H_2:50CO/air$  propagating flames at initial pressure ( $P_u$ ) of 0.1 MPa and equivalence ratio ( $\phi$ ) of 0.8 at different temporal evolutions. In the temperature field shown in Fig. 2a, the red, blue and green (between red and blue) regions represent the burnt, unburned (fresh) gases, and the reacting zone (flame front) respectively. After ignition, the flame front propagated outward spherically until it touched the wall, like the propagating flame observed in the experiment [4–6]. The maximum temperature was around 2200–2500 K, which is in agreement with the adiabatic flame temperature of 2211.4 K. Figure 2b shows that

the velocity was greatest at the flame front, where the chemical reaction occurred. It is noteworthy that the fresh gas velocity at the entrance of the preheat zone of the flame front (green color), i.e. the right outward regime of the flame front, was higher than the velocity of the fresh gas far upstream (blue), indicating that the propagating flame pushed away the fresh gas at the preheat zone of the flame front. This phenomenon was reported in a spherically propagating flame [7] and in a propagating edge-flame in a slot burner [8].

### 3.2. Effect of equivalence ratio

Figure 3 shows simulated pressure histories during combustion of 50H<sub>2</sub>:50CO/air premixed flames at the initial pressure of 0.1 MPa and various equivalence ratios. Maximum explosion pressure increased from lean ( $\phi = 0.8$ ) to equivalence ratio of 1.2, then decreased significantly when mixtures were rich, indicating that maximum explosion pressure occurred at  $\phi = 1.2$ . This occurred because the maximum value of the adiabatic flame temperature for 50H<sub>2</sub>:50CO/air mixture was at  $\phi = 1.2$  causing maximum explosion pressure to occur at the same equivalence ratio. Another interesting point is that the shortest explosion time occurred at  $\phi = 1.6$ . The laminar burning velocity of the 50H<sub>2</sub>:50CO/air mixtures reached the highest value at  $\phi = 2.0$  [9–11]; therefore, the combination of the two effects—the maximum adiabatic flame temperature at  $\phi = 1.2$  and the maximum laminar burning velocity at  $\phi = 2.0$ —caused the explosion time,  $t_c$ , of the 50H<sub>2</sub>:50CO/air mixtures to be shortest at  $\phi = 1.6$ .

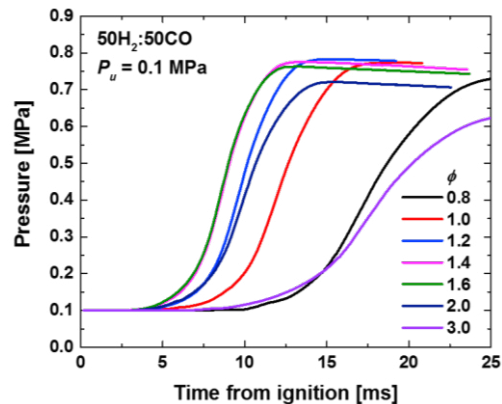


Fig. 3. Explosion pressure of 50H<sub>2</sub>:50CO/air mixtures at various equivalence ratios and initial pressure of 0.1 MPa.

### 3.3. Effect of H<sub>2</sub>:CO ratio

Figure 4 shows simulated pressure histories of various syngas/air mixtures at  $P_u = 0.1$  MPa and  $\phi = 1.0$ . It can be observed that the maximum explosion pressure of syngas/air flames slightly increased with increasing H<sub>2</sub> content in the H<sub>2</sub>/CO fuel blends. The explosion time was significantly influenced by the H<sub>2</sub>/CO ratio, showing that it was shortened by increasing the H<sub>2</sub> content in the fuel blends. The main reason for the shortened ignition time was that the laminar burning velocity of the syngas/air mixture increased quickly with H<sub>2</sub> enrichment in the fuel blends, due to the thermal effect of increasing heat release, thereby increasing the adiabatic flame temperature for H<sub>2</sub> enrichment [12]. Although the differences in  $P_{\max}$  among these mixtures were not significant, it can be expected that the pressure rise rate for mixtures with high H<sub>2</sub> content is much greater than with low H<sub>2</sub> content mixture, due to faster explosion time.

### 3.4. Effect of initial pressure

Figure 5 shows normalized pressures ( $P/P_u$ ) of the 50H<sub>2</sub>:50CO/air premixed flames at  $\phi = 0.8$ , with various  $P_u$ . It can be observed that pressure rise during combustion is very sensitive to the initial pressure change of the mixture. Because self-acceleration of the flame, caused by flame front instabilities at elevated pressures conditions, was the dominant factor in turbulent propagating flames, it increased the maximum explosion pressure and shortened the

explosion time. However, ANSYS Fluent predicted an opposite trend of explosion time at elevated pressures. In this study, the same ignition conditions (location, size and temperature) were used to ignite all mixtures, regardless of the initial pressure. It is expected that the ignition conditions could have a strong influence in the early propagating flame, affecting the explosion time of the flame at elevated initial pressures. Therefore it will be necessary to study the effects of the ignition conditions which may affect propagating flames at elevated pressures.

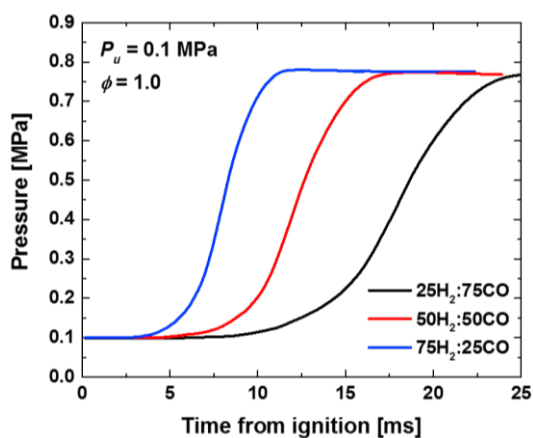


Fig. 4. Explosion pressure of various H<sub>2</sub>:CO/air mixtures at initial pressure of 0.1 MPa and equivalence ratio of 1.0.

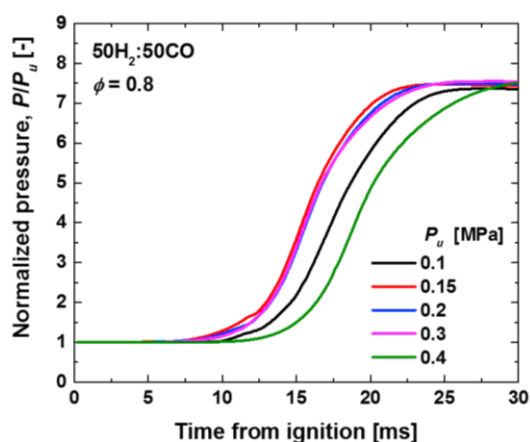


Fig. 5. Explosion pressure of 50H<sub>2</sub>:50CO/air mixtures at various initial pressures and equivalence ratio of 0.8

#### 4. Concluding remarks

In this study, explosion characteristics of various syngas/air flames at different equivalence ratios, H<sub>2</sub>:CO ratios and initial pressures, were numerically investigated to evaluate the hazard of the explosion of syngas/air mixtures. The major conclusions of the study are as follows:

1. The maximum explosion pressure occurs at  $\phi = 1.2$ , while the explosion time is shortest at  $\phi = 1.6$ .
2. The maximum explosion pressure slightly increases, while the explosion time is significantly shortened by increasing H<sub>2</sub> content in the fuel blend.
3. Normalized peak pressure increases with increased initial pressure.
4. Effects of Fluent setting conditions—especially ignition conditions—must be studied further to predict better the explosion of propagating flames at elevated pressures.

#### References

- [1] Richardson Y, Blin J, Julbe A. "A short overview on purification and conditioning of syngas produced by biomass gasification: Catalytic strategies, process intensification and new concepts." *Progress in Energy and Combustion Science* 38 (2012): 765–781.
- [2] Hu K, Zhao Y. "Numerical simulation of internal gaseous explosion loading in large-scale cylindrical tanks with fixed roof." *Thin-Walled Structures* 105 (2016): 16–28.
- [3] Davis SG, Joshi AV, Wang H, Egolfopoulos F. "An optimized kinetic model of H<sub>2</sub>/CO combustion." *Proceedings of the Combustion Institute* 30 (2005): 1283–1292.
- [4] Vu TM, Park J, Kwon OB, Kim JS. "Effects of hydrocarbon addition on cellular instabilities in expanding syngas–air spherical premixed flames." *International Journal of Hydrogen Energy* 34 (2009): 6961–6969.
- [5] Vu TM, Park J, Kwon OB, Bae DS, Yun JH, Keel SI. "Effects of diluents on cellular instabilities in outwardly propagating spherical syngas–air premixed flames." *International Journal of Hydrogen Energy* 35 (2010): 3868–3880.
- [6] Vu TM, Park J, Kim JS, Kwon OB, Yun JH, Keel SI. "Experimental study on cellular instabilities in hydrocarbon/hydrogen/carbon monoxide–air premixed flames." *International Journal of Hydrogen Energy* 36 (2011): 6914–6924.
- [7] Varea E, Modica V, Vandel A, Renou B. "Measurement of laminar burning velocity and Markstein length relative to fresh gases using a new postprocessing procedure: Application to laminar spherical flames for methane, ethanol and isooctane/air mixtures." *Combustion and Flame* 159 (2012): 577–590.

- [8] Tran M-V, Cha MS. “Correction of edge-flame propagation speed in a counterflow, annular slot burner. *Combustion and Flame* 162 (2015): 4671–4672.
- [9] McLean IC, Smith DB, Taylor SC. “The use of carbon monoxide/hydrogen burning velocities to examine the rate of the CO + OH reaction.” *Proceedings of the Combustion Institute* 25 (1994): 749–757.
- [10] Prathap C, Ray A, Ravi MR. “Investigation of nitrogen dilution effects on the laminar burning velocity and flame stability of syngas fuel at atmospheric condition.” *Combustion and Flame* 155 (2008):145–160.
- [11] Sun H, Yang SI, Jomaas G, Law CK. “High-pressure laminar flame speeds and kinetic modeling of carbon monoxide/hydrogen combustion.” *Proceedings of the Combustion Institute* 31 (2007): 439–446.
- [12] Park O, Veloo PS, Burbano H, Egolfopoulos FN. “Studies of premixed and non-premixed hydrogen flames.” *Combustion and Flame* 162 (2015): 1078–1094.